International Journal of Heat and Mass Transfer 257 (2026) 128240

Contents lists available at ScienceDirect

International Journal of Heat and Mass Transfer

journal homepage: www.elsevier.com/locate/ijhmt

Application of the homogeneous relaxation model for flash boiling under sub-atmospheric pressures

Mahmut D. Mat *, Dietmar Kuhn, Abdalla Batta

Institute for Thermal Energy Technology and Safety (ITES), Karlsruhe Institute of Technology (KIT), Hermann-von-Helmholtz-Platz 1, D-76344 Eggenstein-Leopoldshafen, Germany

ARTICLE INFO

Keywords:
Flash Boiling
Converging-diverging nozzle
Homogenous relaxation model (HRM)
Two-phase flow
Pressure undershoot

ABSTRACT

Flashing two-phase flows under sub-atmospheric outlet conditions in a converging–diverging nozzle are investigated using the Homogeneous Relaxation Model (HRM) within a two-phase mixture flow framework. The main objectives of this study are to conduct an in-depth investigation of low-temperature, low-pressure flash evaporation, which is essential in flash-based wastewater purification and power generation systems that utilize low-grade waste heat as an energy source, and to support the improvement of a proof-of-concept experimental setup currently being established in our laboratory through the findings of this study.

The numerical results demonstrate that the mathematical model accurately reproduces pressure and void fraction distributions reported in the literature. It also captures key flashing features—including pressure undershoots, vapor generation delays, and pressure recovery—through the relaxation-time formulation. The results indicate that flashing flow in a converging–diverging nozzle is characterized by a sharp pressure drop near the throat, followed by rapid vapor generation and partial pressure recovery in the diverging section. This behaviour is primarily governed by nozzle geometry and the large disparity in specific volumes between the liquid and vapor phases. Vapor generation increases markedly at higher inlet pressures and temperatures, driven by the greater availability of superheat energy. The simulations further reveal that the mass flow rate is highly sensitive to inlet conditions: elevated inlet temperatures intensify vapor generation and consequently reduce mass flow rate, whereas achieving both high vapor production and high mass flow rates requires sufficiently high inlet pressures. The model also predicts shorter flash-delay distances at higher pressures, indicating an earlier onset of phase change, while longer delays occur at elevated temperatures due to increased metastability. Additionally, pressure undershoots become more pronounced with higher inlet temperatures, whereas their dependence on inlet pressure is negligible. It is found that, under fixed inlet conditions, lower sub-atmospheric back pressures enhance steam generation and promote pressure recovery after the nozzle throat, while simultaneously reducing the mass flow rate and the magnitude of pressure undershoots.

1. Introduction

Flash boiling refers to the rapid phase change that occurs when a hot liquid is suddenly exposed to a pressure lower than its saturation pressure. Unlike conventional boiling, flash boiling happens almost instantaneously, resulting in a high rate of phase change. While this phenomenon is undesirable in some situations such as in the cooling cycles of nuclear reactors or the accidental rupture of tanks containing high-temperature liquids, it is widely utilized in many industrial processes such as paper drying, fuel atomization, and thermal desalination due to its efficiency and cost-effectiveness [1–5]. In geothermal systems, flash evaporation is commonly employed to convert high-temperature liquid water into steam in an efficient and economical manner [3]. Moreover, when coupled with solar thermal collectors, flash evaporation presents a promising method for seawater desalination, offering a sustainable and energy-efficient solution for clean water production [5].

The main advantage of flash boiling is its ability to generate steam solely by reducing the pressure of water, without requiring any additional heat input. This principle creates new opportunities for harnessing low-temperature waste heat from industrial facilities—an energy source traditionally regarded as unsuitable for applications beyond space heating. Flash-based systems provide a practical means of

* Corresponding author.
E-mail address: mahmut.mat@kit.edu (M.D. Mat).

https://doi.org/10.1016/j.ijheatmasstransfer.2025.128240
Received 24 September 2025; Received in revised form 1 December 2025; Accepted 7 December 2025
Available online 14 December 2025

converting otherwise unused thermal energy into steam. Moreover, such systems can simultaneously treat industrial wastewater, enabling the co-generation of electrical power and high-purity water suitable for drinking or industrial use [6]. This dual benefit makes flash systems a promising approach for improving both energy and water efficiency in industrial processes. To advance this concept, a proof-of-concept experimental setup is currently being prepared in our laboratory to enable detailed investigations of flash-based water purification and electricity production using waste heat as energy source.

In a flash power system, the required pressure drop can be achieved through an expansion valve or a converging–diverging nozzle. This rapid reduction in pressure converts initially subcooled water into a metastable or superheated liquid, creating favourable conditions for rapid evaporation [7]. The amount of steam generated and the resulting mass flow rate downstream of the valve or nozzle are key parameters that determine the overall system efficiency. In flash-based power generation or wastewater purification applications, accurately estimating the mass flow rate is essential for effective design and reliable operation. The mass flow rate depends on several factors, including the inlet pressure and temperature, the initial vapor volume fraction, and the magnitude of the applied depressurization. The presence of a vapor phase at the inlet reduces the average density of the two-phase mixture downstream of the nozzle or valve. This lower density favours flow deceleration, thereby reducing the mass flux through the system. As a result, although a higher steam volume fraction indicates more steam production, it also leads to a lower mass flow rate, limiting the total amount of steam transported. Therefore, a thorough understanding of two-phase flow behaviour is essential for optimizing steam generation and minimizing the pumping power required—both of which are critical to the overall efficiency of the system.

Due to the significance of flashing flows in various industrial applications, numerous numerical studies have been carried out to achieve a detailed understanding of flash evaporation and two-phase flow, particularly in converging–diverging nozzles. Since flashing inherently involves the simultaneous presence of liquid and vapor phases, the most advanced mathematical representations typically adopt a two-phase formulation, commonly referred to as the two-fluid model [8–10]. These models solve separate continuity, momentum, and energy equations for each phase, while accounting for complex interphase interactions. Such interactions include drag and lift forces, buoyancy effects, as well as heat and mass transfer across the liquid–vapor interface. This detailed modelling is essential for accurately capturing the dynamics of flashing flows and improving the design and performance of related systems. In their seminal study, Liao and Lucas [8], investigated flashing flow in a converging-diverging nozzle using two-fluid equations that incorporated both drag and non-drag interfacial forces. Phase change was modelled as a result of interphase heat transfer, while pressure-induced phase change was not considered. The simulation results were compared with the experimental data of Abuaf et al [11], and the mathematical model was found to predict the measurements with reasonable accuracy. However, the model had limitation in capturing the pressure recovery after the diverging section of the nozzle and the radial distribution of void fraction. These discrepancies were attributed to the absence of lift force modelling.

In a subsequent study, Liao and co-workers [9] incorporated several wall nucleation models and re-evaluated the predictions against the challenging experiments by Abuaf et al [11]. Nucleation was assumed to occur at the walls of the computational domain. Compared to the previous study that employed a homogeneous nucleation model, the wall nucleation approach showed improved agreement with experimental data. While the homogeneous model tended to overpredict the radial void fraction profile, the heterogeneous models were found to slightly underpredict it.

Despite their potential advantages, two-fluid models face significant challenges related to closure. These models are inherently complex and rely on numerous empirical closure relations, many of which include adjustable numerical constants. Some of these parameters can strongly influence the simulation outcomes, yet they are often difficult to determine accurately and are typically not universal—being valid only for the specific conditions under which they were originally derived. This sensitivity to poorly characterized parameters can undermine the predictive accuracy and general applicability of two-fluid models, particularly in scenarios where experimental data for calibration are limited or uncertain.

An alternative approach for modelling flashing flow is the Homogeneous Equilibrium Model (HEM) or two-phase mixture models. In these models, the two phases are assumed to be in both thermodynamic and mechanical equilibrium, allowing the system to be treated as a pseudo-single-phase flow [12–16]. The model assumes thermal equilibrium and equal velocity for both phases, meaning that no slip occurs between them. For flashing systems, the thermophysical properties of the mixture are determined by the local temperature and pressure. One key advantage of the two-phase mixture approach is that it eliminates the need for an explicit interphase drag models. By assuming infinitely fast momentum exchange between the phases, the model avoids the numerical challenges associated with high drag rates and tightly coupled phase velocities—issues that often lead to high computational costs and potential numerical instabilities in two-fluid models. However, the primary drawback of the homogeneous approach is the risk of overpredicting interphase momentum transfer, which can lead to inaccuracies in certain flow regimes where slip effects are significant.

A notable example of the mixture modelling approach is the pioneering study by Maxsic and Mewes [12], in which they simulated flashing flows in pipes and nozzles using a simplified two-fluid framework implemented within the commercial CFD code CFX 4.2. In their formulation, both phases were assumed to share a common velocity field. The model included separate continuity equations for the liquid and vapor phases, a single momentum equation for the mixture, and an energy equation applicable to the liquid phase only. The vapor phase was assumed to remain saturated throughout the flow, while interfacial heat transfer was modelled as being primarily driven by thermal conduction.

In a comprehensive study, Le et al. [13] employed a mixture model that incorporates a drift velocity, representing the relative motion between the vapor phase and the bulk mixture. This approach enables a more accurate representation of phase slip in two-phase flows. The phase change process was modelled using a formulation based on the difference between the vaporization pressure and the local vapor partial pressure, allowing for a realistic prediction of vapor generation. To account for thermal non-equilibrium effects, a simplified boiling delay model was introduced, capturing the time lag between the onset of thermodynamic boiling conditions and the actual initiation of phase change.

Various models have been employed in mixture-based two-phase flow simulations to account for mass exchange between the vapor and liquid phases. However, most of these models fall short in accurately representing complex phenomena inherent in flashing flows, such as pressure undershoots and delays in vapor generation. To address these limitations, the Homogeneous Relaxation Model (HRM) is adopted in this study as a more promising approach. The potential usefulness of the Homogeneous Relaxation Model (HRM) for describing mixture two-phase flows was first suggested by Bilicki and Kestin [17]. Its principal advantage lies in its ability to capture wave dispersion and dissipation phenomena more simply than traditional two-fluid models. The most significant dispersive effects were found to arise from the thermodynamic disequilibrium between the liquid and vapor phases, particularly due to the finite rate of interphase mass transfer. This is especially relevant when the liquid enters a metastable state before undergoing phase change. Schmidt et al [18] successfully applied the HRM to simulate steady flashing flow in channels. Their numerical predictions demonstrated good agreement with experimental data, highlighting the capability of the HRM to accurately capture the essential physics of

flashing flows while maintaining a manageable level of model complexity.

The Homogeneous Relaxation Model (HRM) is primarily employed in the modelling of fuel atomization processes, particularly in gasoline direct injection (GDI) engines and similar high-pressure applications [19]. However, its application to flashing phenomena involving water under low-pressure conditions—such as those found in vacuum or near-atmospheric environments—has not yet been explored. Therefore, this study aims to bridge that gap by adapting and integrating the HRM into a mixture-based two-phase flow framework using the Volume of Fluid (VOF) method. The objective is to develop a cost-effective and computationally efficient tool capable of accurately capturing the flashing behaviour within a converging-diverging nozzle. In particular, the study focuses on evaluating the influence of key process parameters—especially mass flow rate—on the characteristics and dynamics of the flashing flow.

Although numerous numerical studies have investigated flashing flows, most have focused on conditions with relatively high inlet and outlet pressures and temperatures. Comprehensive analyses under atmospheric or sub-atmospheric (vacuum) conditions remain limited, representing a notable gap in the literature. This gap is particularly important given the relevance of vacuum flashing in flash-based water purification and power generation systems, which aim to simultaneously purify wastewater and generate electricity by utilizing low-temperature waste heat—an abundant yet often underutilized energy source in industrial environments. A clear understanding of flashing behaviour at low pressures is essential for optimizing the efficiency and practical viability of such sustainable energy technologies. Furthermore, although flashing is inherently a highly non-isothermal process due to rapid phase change and the associated latent heat effects, temperature distributions within flashing flows have received comparatively little attention. Most existing studies emphasize pressure profiles and vapor volume fractions while overlooking the thermal field, which plays a critical role in both the initiation and progression of flashing.

To address these gaps, this study investigates flash boiling in a converging–diverging nozzle under sub-atmospheric outlet conditions and relatively low inlet pressures and temperatures using a compact two-phase mixture model integrated with the Homogeneous Relaxation Model (HRM). The model is first validated against experimental data from the literature and then applied to examine the influence of operating parameters—such as inlet pressure and temperature—on vapor generation, pressure distribution, mass flow rate, and critical flashing features including pressure undershoots and flash-delay distances under sub-atmospheric back pressure conditions.

2. Mathematical modeling

Flash boiling is investigated in a converging-diverging nozzle, as illustrated in Fig. 1. This geometry is selected due to its practical relevance in various engineering applications and its ability to isolate the flash boiling phenomenon from complications arising in more complex geometries. The simplified structure of the nozzle enables a focused analysis of the flashing process. Additionally, the use of this geometry facilitates direct comparison with numerous existing experimental and numerical studies, allowing for meaningful validation of the current results against published data.

Instead of solving separate sets of equations for each phase, the Volume of Fluid (VOF) model is employed to represent flash boiling as a mixture model. This approach eliminates the need to explicitly model numerous interfacial interactions, allowing the numerical study to focus more directly on vapor generation resulting from the sudden pressure drop induced by the converging section of the nozzle. Therefore, VOF method offers a practical balance between computational efficiency and the ability to capture key phase change dynamics in flashing flows.

The Volume of Fluid (VOF) model, originally introduced by Hirt and Nichols [20], is implemented in the multiphase modelling framework of STAR-CCM+ [21]. VOF is a relatively simple yet effective multiphase advection model that tracks the interface between phases by solving for the volume fraction of each phase within computational cells. In this approach, all phases are assumed to share common pressure, velocity, and temperature fields. As a result, the governing equations for mass, momentum, and energy take the same form as in single-phase flow, but are solved using mixture properties that are weighted by the local volume fractions.

Thus, following equations governing mass momentum energy conversation along with phase change are solved in this study;

Continuity equation

$$\frac{\partial \rho}{\partial t} + \nabla.(\rho \boldsymbol{V}) = 0 \tag{1}$$

Momentum Equation

$$\frac{\partial (\rho \boldsymbol{V})}{\partial t} + \nabla.(\rho \boldsymbol{V}\boldsymbol{V}) = -\nabla p + \nabla.(\boldsymbol{T}) + \rho g + \boldsymbol{F} \tag{2}$$

Energy Equation

$$\frac{\partial (\rho h)}{\partial t} + \nabla.(\rho h \boldsymbol{V}) = \frac{\partial p}{\partial t} + \nabla.(k \nabla T) + (T.\nabla)V + S_h \tag{3}$$

Volume fraction of vapor

$$\frac{\partial \alpha_v}{\partial t} + \nabla.(\alpha_v \rho_v V) = S_M \tag{4}$$

where ρ, V, h, k are mixture density, velocity, enthalpy and conductivity which represent each phase by their volume fraction, $\boldsymbol{T}$ denotes the viscous stress tensor, S_h source term representing energy transfer between two phases, S_M is the source term representing vapor

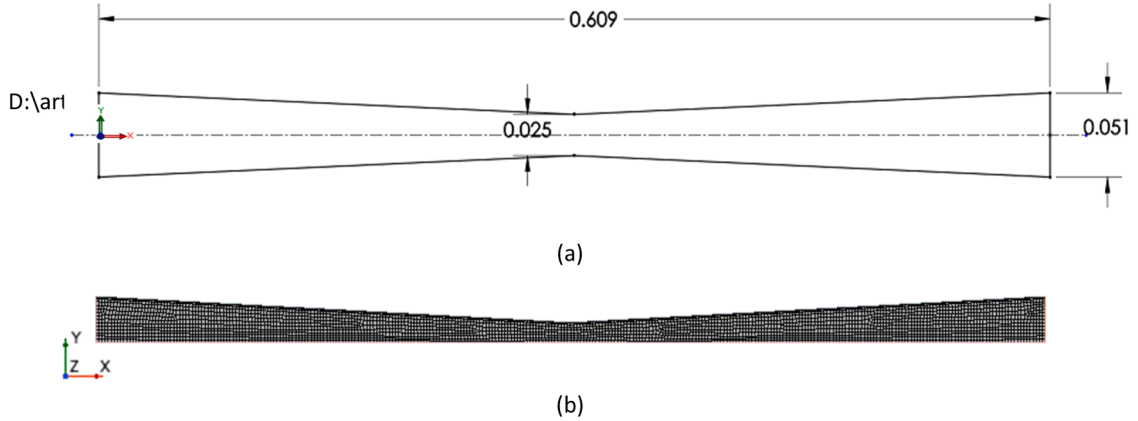

Fig. 1. (a) Geometry (all units are in m) and (b)grid system of the problem considered.

generation, which is calculated using the Homogeneous Relaxation Method as described in the subsequent section.

2.1. Homogenous relaxation model (HRM)

The Homogeneous Relaxation Model, introduced by Bilicki and Kestin [17], is employed to predict vapor generation in flashing flows. The HRM is based on the assumption that thermal equilibrium between the liquid and vapor phases is not instantaneous but is established after a finite characteristic time, referred to as the relaxation time. During this relaxation period, the system transitions toward thermodynamic equilibrium, allowing the model to account for the delayed phase change that occurs in rapid depressurization processes in the flash boiling.

The HRM method calculates the rate of change of vapor mass fraction using an exponential time-scale formulation, where the source term represents vapor generation as follows;

$$S_M = -\rho_{mix}\frac{x_e - x}{\theta} \tag{5}$$

where θ is the relaxation time scale, ρ_{mix} is the mixture density, x is the mass fraction of the vapor phase and x_e is the equilibrium mass fraction of the vapor and calculated using following equation

$$x = \frac{h - h_{sat,l}}{h_{sat,v} - h_{sat,l}} \tag{6}$$

Where h is the mixture specific enthalpy while h_{sat} are the vapor and liquid specific enthalpies at the saturated conditions.

The relaxation time scale proposed by Downar-Zapolski at al [22] and defined as:

$$\theta = \theta_0 \alpha_v^a \varphi^b \tag{7}$$

Where α_v is the volume fraction of the vapor, a and b are empirical constants take the values of -0.54 and -1.76 at low pressures below 10 bar and above 10 bar take the values. φ is the non-dimensional pressure and calculated as:

$$\varphi = \frac{P_{sat} - P}{P_{crit} - P_{sat}} \tag{8}$$

where P_{crit} is the critical pressure of water and P_{sat} is the saturation pressure. The Antoine equation is used to calculate the saturation pressure of the fluid as a function of temperature and is given by:

$$log_{10}(P_{sat}) = A - \frac{B}{C + T} \tag{9}$$

where P_{sat} is the saturation pressure, T is the temperature (°C), and A, B, and C are empirical constants specific to the fluid. The values of the parameters used in the HRM and Antoine equations are presented in Table 1.

The relaxation parameter θ (Eq.7] introduced in the Homogeneous Relaxation Model (HRM) governs the rate at which the liquid–vapor mixture approaches thermodynamic equilibrium. This parameter captures the finite response time of the phase change process. As a result, even when local thermodynamic conditions favour vapor formation—i.e., when the pressure drops below the saturation pressure—the actual vapor content lags behind the equilibrium value. A larger θ implies a slower relaxation process, leading to more pronounced pressure undershoots and a delayed onset of observable vapor generation. This feature makes HRM well-suited for capturing non-equilibrium effects in rapid depressurization in flashing scenarios.

Table 1
Values of parameters used in the calculations.

Parameter	Value
P_{crit}	2.2055E7 Pa
T_{crit}	647.12 K
a (Eq. (7))	-0.54
b (Eq. (7))	-1.76
A (Eq.9)	11.949
B (Eq. (9))	3978.205
C (Eq.9)	-39.801

The second term (α_v^a) in the relaxation time expression (Eq.7] used in the HRM framework can be interpreted as representing nucleation effects. In previous studies, nucleation has been modelled either through a constant bubble density assumption or more detailed microscopic nucleation models. This term reflects the sensitivity of the vapor generation rate to the local void fraction, and its inclusion captures the nonlinear behaviour observed during phase change initiation. Nucleation is considered the most energetically demanding stage of vapor formation, as it requires overcoming the interfacial tension to form stable vapor bubbles. The energy barrier and stochastic nature of nucleation make it one of the most complex and uncertain aspects of modelling flashing flows.

According to the Downar–Zapolski (DZ) equation [Eq. (7)], no vapor generation occurs as α→0, reflecting the absence of initial vapor nuclei. However, once a small amount of vapor is present, vapor generation becomes increasingly easier—this behaviour corresponds to the onset of nucleation. The exponent a in the relaxation time formulation can be adjusted to represent different degrees of nucleation resistance. For instance, setting a=0 implies no nucleation delay, meaning that flashing initiates instantaneously once a nonzero void fraction ϕ appears. In contrast, larger negative values of a, such as a=−0.3, correspond to moderate nucleation resistance, while smaller values (e.g., a=−0.5 or −0.7) indicate stronger nucleation effects and a delayed onset of vapor formation. Since the influence of this parameter has been extensively examined in earlier studies, the constant values used in this work are adopted as recommended by Downar- Zapolski et al [22].

2.2. Turbulence modeling

The local Reynolds number (Re) calculated based on the average mass flow rate in the nozzle above 10^5 indicating fully turbulent flow for all cases considered in this study. Therefore, the realizable k-ε turbulence model [23] is selected, as it is widely used in similar flow regimes and offers a good compromise between robustness, computational cost, and accuracy. This model performs reliably across both fine and coarse mesh resolutions, making it well-suited for the current numerical investigation.

Turbulence boundary conditions at the nozzle inlet are specified by imposing a constant turbulence intensity. A range of turbulence intensity values is tested to evaluate their influence on the flow predictions. Among the values examined, a turbulence intensity of 1% yields the best agreement with the experimental data and is therefore adopted for all subsequent simulations.

2.3. Numerical implementation

The computational domain is discretised using structured quadrilateral elements, with prism layers applied near the walls to accurately capture boundary layer effects (Fig.1b). An outlet static pressure boundary condition is imposed to induce an additional pressure drop beyond that caused by the geometric contraction at the throat of the converging-diverging nozzle. This setup allows for better control of the downstream flow behaviour and supports the development of flashing conditions within the nozzle.

To reduce computational cost, a two-dimensional axisymmetric model of the nozzle was developed (Fig. 1b), assuming no variation in the tangential direction. In STAR-CCM+, the axisymmetric configuration corresponds to a 1-radian sector in the circumferential (θ) direction, with the solver performing the computations in a three-dimensional framework[21]. The lower boundary of the computational domain represents the axis of symmetry, where the *axis* boundary condition is

applied. In all simulations, both pressure and temperature are prescribed at the inlet, while only the pressure is specified at the outlet. The void fraction at the inlet is set to a small value ($\alpha=10^{-5}$) to ensure numerical stability. For the same reason, the initial vapor volume fraction throughout the entire computational domain is also set to $\alpha=10^{-5}$. No-slip and adiabatic boundary conditions are applied at the nozzle walls, implying that any temperature drop within the system arises solely from the energy consumed during the phase change of liquid water into vapor. A symmetry boundary condition is applied along the nozzle axis. A range of inlet temperatures and pressures, as well as outlet pressures, are considered in the simulations. The operational conditions and the specific cases analysed are summarized in Table 2.

Although the flow is inherently steady, the critical nature of flashing phenomena requires the use of a quasi-steady approach in the numerical simulations. A very small-time step (10^{-4}) is employed to satisfy the Courant–Friedrichs–Lewy (CFL) condition and to ensure numerical stability. The simulations are run until a steady-state solution is achieved, at which point the flow variables no longer exhibit temporal variations. Only the final steady-state results are presented and discussed in this study.

To improve convergence and stability, an initial velocity and pressure field is first obtained by solving a turbulent single-phase flow in the same geometry, using identical inlet conditions for pressure and temperature. Once the single-phase solution converges, the resulting velocity, pressure, and temperature fields are used as the initial conditions for the two-phase flashing flow simulations. This approach provides a well-initialized flow field, which significantly enhances convergence behaviour. As a result, a well-converged solution is achieved for all cases considered in this study. The solution iterations are terminated after the mass balance between inlet and outlet less than 10^{-4} kg/s and the maximum residual of all equations below 10^{-6}.

A grid independence study is conducted using several mesh configurations, ranging from coarse to very fine grids. Key flow parameters within the nozzle are monitored for each grid system to evaluate the sensitivity of the numerical results to mesh resolution. Fig. 2 presents the predicted average vapor void fraction distributions along the nozzle for the different mesh sizes tested. It is seen that even very coarse grid system of 546 cells numerical solution can capture the main physics of flash boiling. The results indicate that the calculated void fractions do not change after a moderate grid system further and grid refinement has a negligible effect on the predicted void fractions. Based on this observation, a medium-resolution mesh consisting of 4249 cells is selected for the present study, offering a suitable balance between computational cost and solution accuracy.

3. Results

The accurate estimation of void fraction, mass flow rate, velocity, and temperature distributions near expansion valves or nozzles is crucial for both efficient system design and safety assurance in flash boiling based power and pure water production systems. In this study, a simple yet effective approach for representing flash boiling in a converging-diverging nozzle is investigated numerically using a compact mixture-fluid formulation coupled with the Homogeneous Relaxation Model (HRM). The accuracy of the mathematical model and the numerical approach is first validated by comparing experimental data. Following validation, the model is applied to investigate flash boiling under vacuum conditions to gain insight into the behaviour of such flows and to generate data relevant for the design of systems operating in low-pressure environments. Table 2 provides a summary of all cases considered in the computations.

Table 2
Cases considered.

	P_{in}(kPa)	T_{in}(K)	P_{out}(kPa)	Note
Case 1	555.9	402.5	422.25	BNL309
Case 2	443.4	101.2	372.85	BNL362
Case 3	110	370	50	
Case 4	110	360	50	
Case 5	150	380	50	
Case 6	150	370	50	
Case 7	150	360	50	
Case 8	150	350	50	
Case9	200	380	50	
Case10	200	370	50	
Case 11	200	360	50	
Case 12	200	350	50	
Case 13	150-200	350-370	20-50	

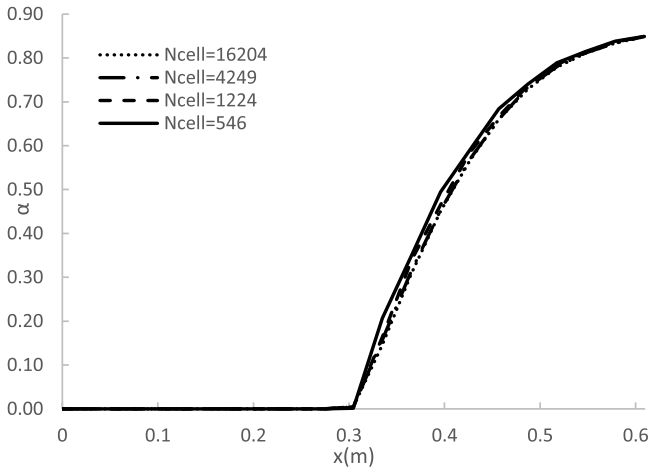

Fig. 2. Grid Independence test.

3.1. Validating numerical results with measurements

To validate the numerical results, experimental data from Abuaf et al [11] are employed. Abuaf and colleagues conducted a comprehensive series of experiments at Brookhaven National Laboratory (USA) to investigate flash boiling phenomena in a converging-diverging nozzle. Their research focused on examining the effects of operating parameters on the mass flow rate of the liquid-vapor mixture at the nozzle outlet. High-precision instruments were used to measure pressure and void fraction at multiple locations along the nozzle. Each test case is labelled with a "BNL" prefix (e.g., BNL309) for ease of reference. In the present work, numerical predictions are compared with representative experimental cases from Abuaf et al [11], specifically BNL309 and BNL362.

Fig.s 3a and 3b compare the predictions of the HRM model with experimental results from BNL309, which is considered the most challenging case due to its high inlet subcooling and elevated pressure. The both figures indicate that the employed mathematical model provides a satisfactory estimation of the experimental data. Fig. 3a presents the predicted void fraction distribution along the nozzle. It is observed that vapor generation does not occur in the first half of the nozzle. Once flashing initiates just after the throat, a rapid increase in vapor formation ensues. Over a short distance, the average void fraction rises sharply, reaching approximately 0.7 at the nozzle exit. The model captures this behaviour well. However, it slightly overpredicts vapor formation in the mid-section of the diverging part, while showing only minor deviation from the experimental data near the outlet. Fig. 3b compares the predicted and measured pressure distributions along the nozzle. A sharp pressure drop is observed near the throat, followed by a gradual flattening of the pressure profile in the diverging section, primarily due to pressure recovery associated with the increasing cross-sectional area of the nozzle and low volumetric density of the vapor phase generated. The model shows excellent agreement with experimental data in the converging section. However, it slightly underestimates the pressure recovery after the onset of flashing in the

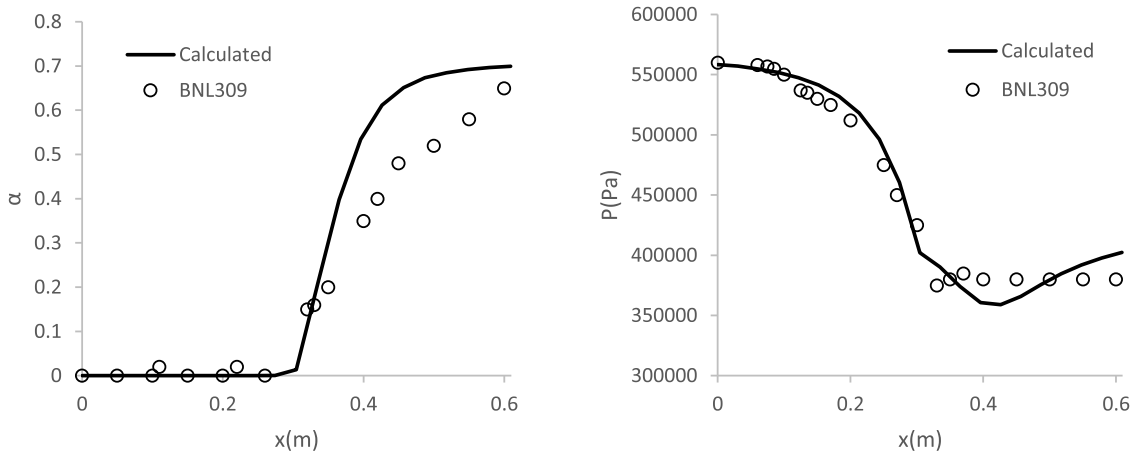

Fig. 3. Comparison of calculated results with experimental data from the literature (BNL309).

diverging part, indicating a limitation of the model in capturing the post-flashing pressure dynamics accurately.

Accurate prediction of mass flow rate is critical in flashing flows, as the presence of two phases and pressure fluctuations significantly influence the overall flow behaviour. For the BNL309 case, the predicted mass flow rate is 8.5 kg/s, while the experimentally measured value is 8.9 kg/s. This corresponds to a deviation of less than 5%, demonstrating that the mathematical model employed in this study provides a highly satisfactory estimation of mass flow rate. Considering potential experimental uncertainties in the mass flow rate measurement, this level of agreement can be regarded as well within an acceptable range.

The predictions of the mathematical model were further validated against another critical experimental case by Abuaf et al [11], referred to as BNL362. Fig. 4a shows that the model successfully captures the void fraction distribution throughout the nozzle. Although a slight overprediction is observed near the outlet section, the discrepancy gradually decreases, and the model estimates the void fraction with satisfactory accuracy in the outlet region.

The predicted and measured pressure distributions for the BNL362 case are compared in Fig. 4b. As with the BNL309 case, the model accurately captures the pressure profile in the converging section of the nozzle. However, it underestimates the pressure in the diverging section, particularly after the onset of significant vapor generation. Despite this deviation, the overall trends in both the predicted void fraction and pressure profiles demonstrate that the model effectively captures the fundamental physical mechanisms governing flashing flow in a nozzle. The model has also been applied to other experimental cases reported by Abuaf et al [11], yielding similarly satisfactory agreement; presentation of these additional comparisons is omitted here for brevity.

3.2. *Numerical Study of Flashing Flow under sub-atmospheric condition*

After validating the two-phase mixture model coupled with the Homogeneous Relaxation Model (HRM), it is applied to investigate flashing phenomena under sub-atmospheric conditions at the nozzle outlet. As previously mentioned, understanding flashing under vacuum is essential for the development of flash-based power generation and water purification systems that utilize low-temperature waste heat as their energy source. The same converging-diverging nozzle geometry is employed to focus solely on the flashing flow under vacuum, avoiding further complexity introduced by different geometrical configurations. This geometry is considered to serve as a representative model for inducing flashing boiling through sudden pressure drops in such systems.

Fig. 5 presents contours of vapor void fraction, pressure, temperature, and axial velocity, providing an overview of the flow parameter distributions within the nozzle for a typical operating condition of the flash-based water purification and power generation system currently under development in our laboratory (P_{init}=150 kPa, T_{init}=370 K, P_{out}=50 kPa, Case-6). Fig. 5a show that vapor formation begins just downstream of the throat and progressively intensifies along the diverging section of the nozzle. This trend is attributed to the continuous accumulation and expansion of the vapor phase as the flow progresses. It is important to note that the vapor distribution shown represents volume fraction, not mass fraction. Due to the significantly lower density of the vapor compared to the liquid phase, even a small amount of vapor mass can occupy a large volume, causing the channel to appear rapidly filled with vapor in the volume fraction representation. The velocity vectors overlapping with the volume fraction contours around the nozzle are also illustrated in this figure to show the evolution of the flow field as vapor formation develops downstream of the throat. Further details of

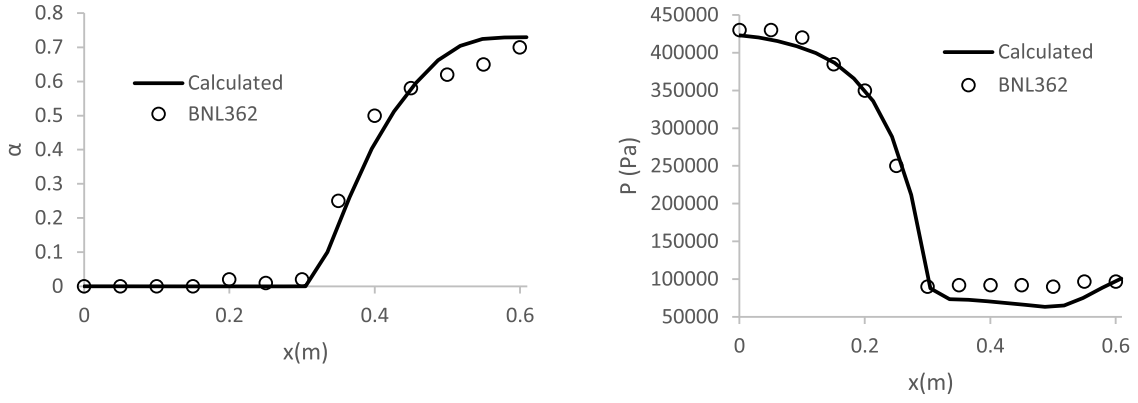

Fig. 4. Comparison of the calculated results with BNL 362.

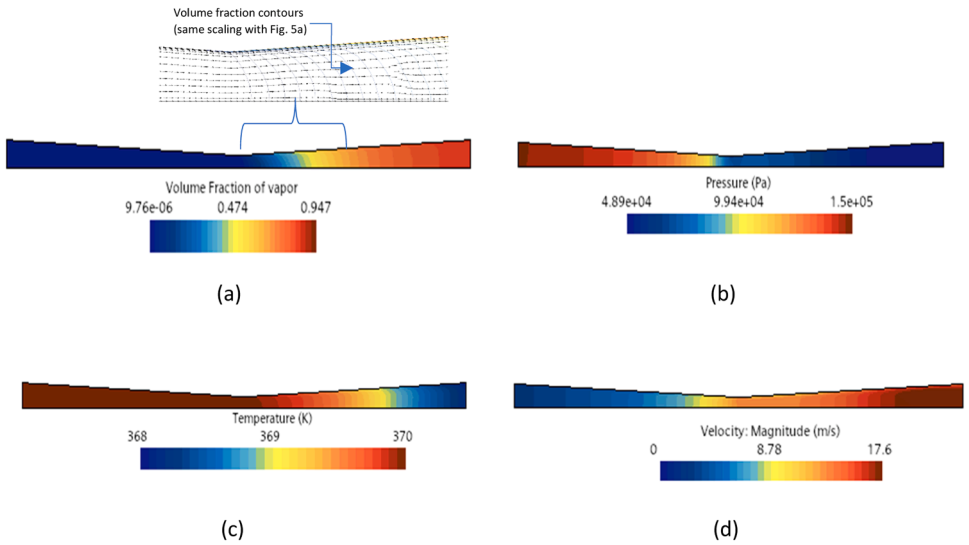

Fig. 5. Calculated (a) void fraction and section with volume fraction contours overlaid with velocity vectors, (b) pressure distribution, (c) temperature contours, and (d) velocity field.

the velocity field are discussed in the subsequent sections.

The pressure distribution within the nozzle is presented in Fig. 5b. It is observed that the inlet pressure is maintained at a prescribed value, and the pressure gradually decreases up to the throat, followed by a sharp drop downstream of the throat. The pressure variation is predominantly in the axial direction, with no discernible change in the radial direction. The temperature distribution along the nozzle is shown in Fig. 5c. As seen in the figure, there is no significant temperature change in the converging section. However, a noticeable temperature drop occurs downstream of the throat, where intense flashing takes place. Given the assumption of adiabatic flow, this temperature reduction is attributed to the energy consumed during the liquid-to-vapor phase transition.

The velocity profile within the nozzle is illustrated in Fig. 5d. It is observed that the liquid accelerates through the nozzle primarily due to the geometric effect of the converging section and the substantial vapor generation occurring in the diverging section. To better highlight the velocity dynamics of the two-phase mixture, the axial velocity distribution along the centreline of the nozzle is presented in Fig. 6 for the same case. The velocity increases almost linearly in the converging section, controlled by the decreasing cross-sectional area. Two distinct acceleration regions are observed downstream of the throat. The first is attributed to the geometric expansion of the diverging section, while the second, more pronounced increase in velocity occurs mid-way through the diverging part, corresponding to intense vapor formation. This secondary acceleration reflects the additional volumetric expansion associated with the phase change from liquid to vapor. Since the density of the vapor phase is significantly lower than that of the liquid, the mixture must accelerate to conserve mass flow rate during the phase transition. This acceleration is particularly evident in the diverging section where intense vapor generation occurs. However, in the downstream region of the diverging part, the velocity begins to decrease due to the continued geometric expansion of the nozzle, which reduces the flow velocity despite the lower mixture density.

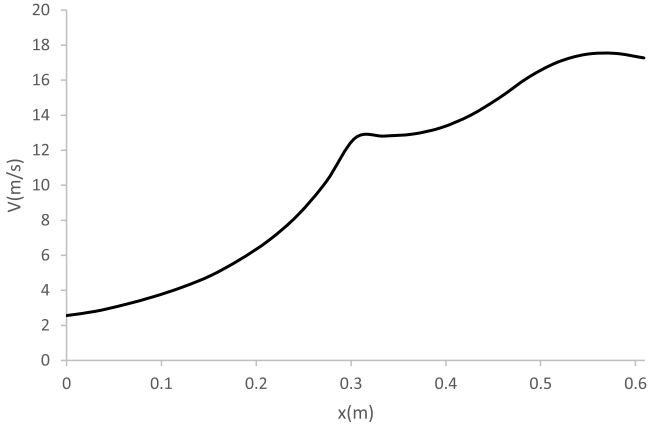

Fig. 6. Calculated mixture velocity and void fraction at the center of the nozzle.

Details of the flashing flow under sub atmospheric conditions for Case-6 (P_{init}=150 kPa, T_{init}=370 K, P_{out}=50 kPa) are presented in Fig. 7, which shows the pressure distribution, void fraction, and the calculated saturation pressure using the Antoine equation (Eq. (9)) at the centerline of the nozzle. The flow begins with subcooled liquid water, where the pressure is initially higher than the saturation pressure. As the water flows through the converging section of the nozzle, the pressure decreases due to the geometric constriction. At the throat of the nozzle, the pressure drops to the saturation pressure, initiating the flashing process. However, flashing does not begin immediately when the fluid pressure drops to the saturation pressure corresponding to its temperature. Instead, an additional pressure drop is typically required to initiate flashing. This is because a temperature gradient between the liquid and vapor phases is necessary to enable heat transfer, which facilitates phase change. Therefore, the onset of flashing is delayed until the thermodynamic and kinetic conditions are sufficient to overcome this energy barrier.

In such condition, the liquid remains in a metastable state—where it is thermodynamically unstable but does not immediately vaporize. This phenomenon is common in rapid expansions, where the fluid does not have sufficient time to undergo phase change instantaneously. The difference between the saturation pressure and the actual pressure at which vaporization begins is referred to as pressure undershoot [8–9,11–13]. The pressure undershoots and flashing delay distance is demarcated on Fig. 7 for clarity. This behaviour results primarily from the inertia of phase change, meaning that the metastable fluid lags behind thermodynamic equilibrium due to finite relaxation times associated with nucleation and vapor growth. This behaviour contrasts significantly with equilibrium boiling, in which vapor forms immediately once the fluid reaches the saturation pressure, with no pressure undershoot observed.

It should be noted that the Homogeneous Relaxation Model (HRM)

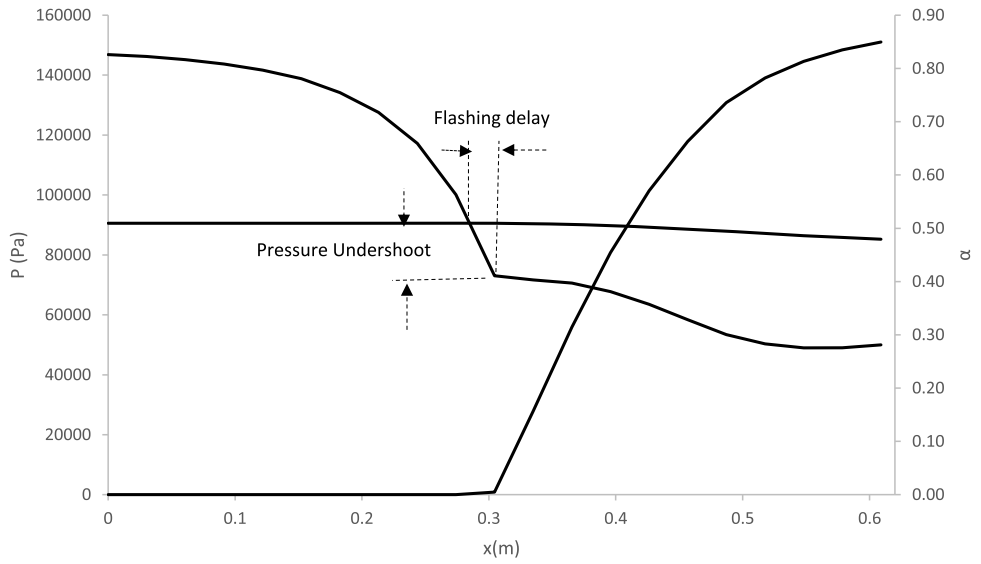

Fig. 7. Calculated Pressure undershoot and flash delay.

does not explicitly determine the flashing inception point as a distinct event. Instead, it assumes that vapor generation begins once a pressure undershoot occurs, initiating a non-equilibrium phase change process. As a relatively simple yet powerful model, HRM does not explicitly model nucleation mechanisms. Rather, it assumes that the metastable liquid begins to relax toward thermodynamic equilibrium once the local pressure, P falls below the saturation pressure $P_{sat}(T)$. The rate of this relaxation—and hence the rate of vapor generation—is governed by a characteristic relaxation time, allowing HRM to approximate the dynamics of flashing without resolving the detailed microphysics of nucleation.

The effects of initial temperature on vapor generation and the resulting pressure dynamics are illustrated in Fig. 8. The average void fraction (Fig. 8a) and pressure (Fig. 8b) along the nozzle are presented in the figure. In this parametric study, the inlet pressure is fixed at 150 kPa, a representative value commonly encountered in wastewater treatment systems that utilize low-temperature waste heat sources. As expected, higher inlet temperatures lead to enhanced vapor generation, since more thermal energy is available to drive the phase change. For all cases considered, the vapor fraction is seen to increase rapidly—almost exponentially—just after the nozzle throat. At lower inlet temperatures, the vapor fraction remains nearly constant until midway through the diverging section, and flashing eventually ceases. This behaviour occurs because the fluid pressure remains above the saturation pressure, and therefore no superheating energy is available to sustain vapor generation. In contrast, at higher initial temperatures—such as 380 K, which is only 2 K below the saturation temperature at 150 kPa—vapor generation initiates shortly after the throat. The vapor fraction then increases rapidly and begins to level off toward the outlet, as most of the liquid has already been converted to vapor.

The pressure distribution (Fig. 8b) follows a similar overall trend across all cases, though the magnitude of the pressure drop varies with the initial temperature. At lower inlet temperatures, the pressure drop is more pronounced due to the limited vapor generation and lower vapor content. In contrast, at higher initial temperatures, the pressure drop is less severe near the throat, owing to the rapid formation and expansion of vapor, which mitigates further pressure reduction. However, a more substantial pressure drop is observed toward the outlet in the highest-temperature case. This can be attributed to the completion of vapor generation and the resulting acceleration of the vapor-dominant flow, which enhances momentum and lowers static pressure downstream.

The calculated velocity profiles depending on the inlet temperature are presented in Fig. 9. It is observed that the mixture velocity increases almost linearly up to the nozzle throat due to the converging geometry. Beyond the throat, during the flash vapor generation, the velocity remains nearly constant. At lower inlet temperatures, the flow velocity is higher up to the mid-section of the diverging part, as less vapor is generated and the liquid phase dominates. However, at higher inlet temperatures, the velocity profile exhibits a different behaviour near the outlet. This change is attributed to the higher vapor content at elevated temperatures, which leads to increased volumetric expansion. As a result, the flow accelerates in order to conserve mass flow rate, causing a noticeable rise in velocity near the outlet section. There is a competing interaction between the increasing flow area and the expansion caused by vapor production. The increase in velocity clearly correlates with temperature, as enhanced vapor generation drives higher mixture velocities. The slight decrease in velocity observed near the outlet is mainly due to the larger cross-sectional area resulting from the diverging geometry of the nozzle.

Similar trends in void fraction and pressure distribution were observed across the other cases considered. These cases, aimed at investigating the effects of varying inlet pressures and temperatures, are summarized in Table 2. Therefore, to avoid redundancy, only the mass flow rates at various inlet pressures and temperatures are presented in Fig. 10. It is evident that the mass flow rate through the nozzle is significantly influenced by both parameters. Higher inlet pressures combined with lower temperatures result in increased mass flow rates. This is due to the higher density and lower specific volume of the liquid phase under these conditions. In contrast, at higher temperatures, the mass flow rate decreases substantially because of the increased vapor content and lower density of the mixture. However, increasing the inlet pressure can counteract this effect and enhance the mass flow rate even at elevated temperatures. For instance, at an inlet temperature of 370 K, raising the pressure from atmospheric to 200 kPa nearly doubles the mass flow rate. This has important implications for applications such as wastewater treatment and waste heat recovery. Nonetheless, it should be noted that while higher inlet pressures improve mass throughput, they also increase the energy required to drive the flow. Therefore, an optimal balance between energy consumption and desired flow rate must be determined based on the specific system requirements.

Pressure undershoots and flash delay distances across a range of inlet pressures and temperatures are compared in Fig. 11. As illustrated in Fig. 11a, pressure undershoots become more pronounced at higher inlet temperatures. This trend is attributed to the increased thermal energy available for superheating, which causes a larger deviation from thermodynamic equilibrium prior to the onset of flashing. In contrast, the

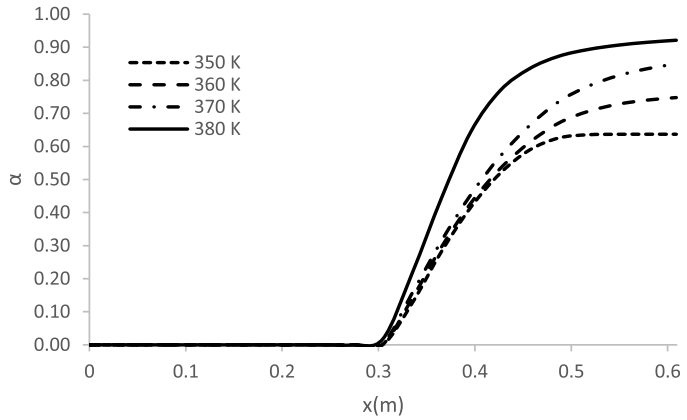

(a)

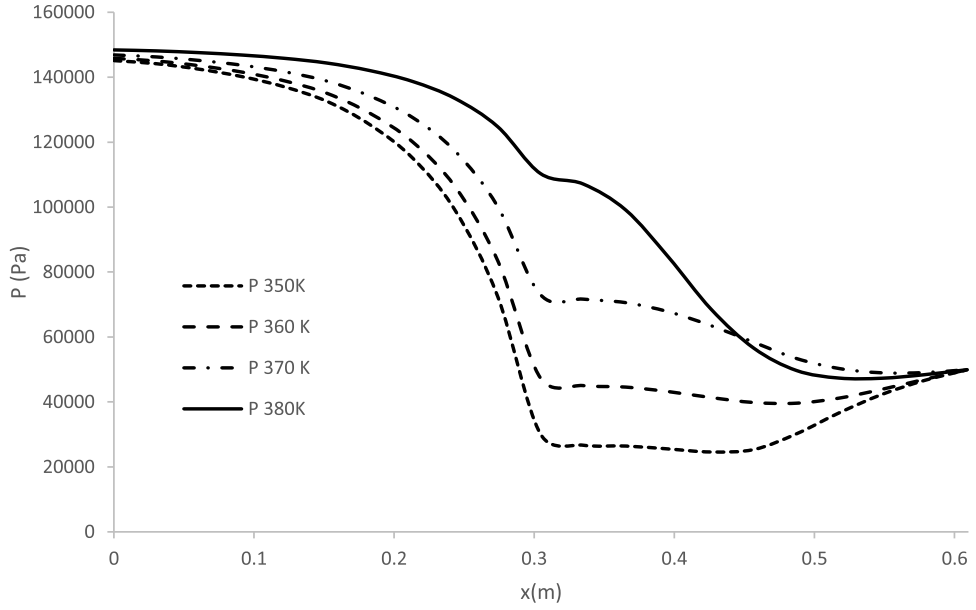

(b)

Fig. 8. Effects of initial Temperature on (a) void fraction (b) pressure distribution (P_{inlet}=150 kPa).

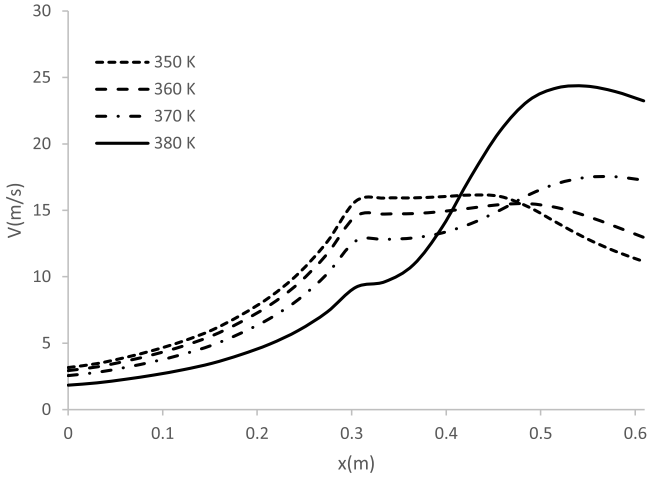

Fig. 9. Effects of Initial temperature on mixture velocity at the center of nozzle.

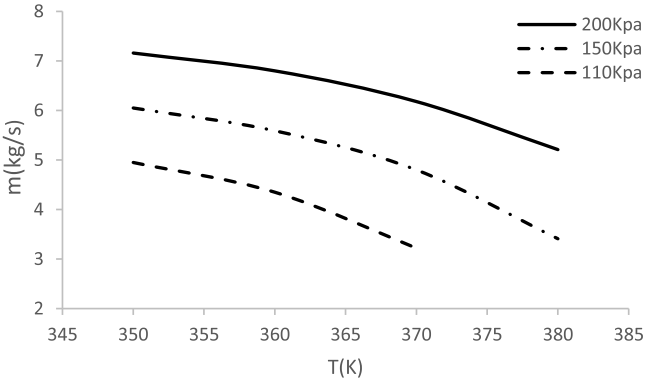

Fig. 10. Effects on inlet temperature and pressure on the mass flow rate.

influence of inlet pressure on pressure undershoots appears negligible. This may be due to the shifting saturation pressure with temperature, leading to undershoots occurring at different absolute pressure levels for

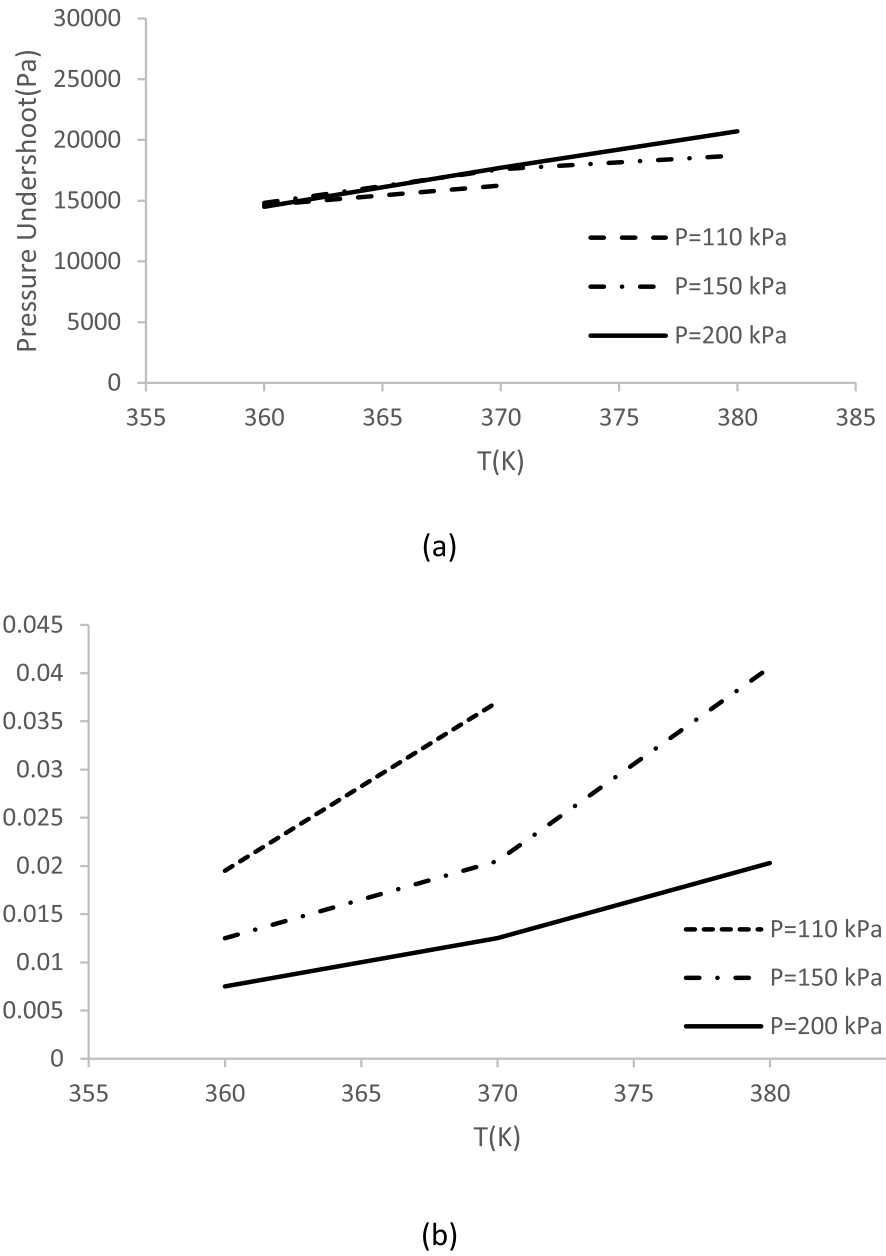

Fig. 11. Effects of inlet temperature and pressure on flashing delay and pressure undershoots.

each case. Fig. 11b demonstrates that flash delay distance decreases with increasing inlet pressure, but increases with higher inlet temperatures. This indicates that while superheating is more intense at elevated temperatures, the initiation of flashing is delayed—likely due to enhanced metastability and increased nucleation resistance under those conditions.

The flashing behaviour under sub-atmospheric conditions was further examined by reducing the outlet pressure from 50 kPa to 20 kPa in 10 kPa increments in Fig. 12. Outlet pressures below 20 kPa were not considered because the flash power-generation and water-purification system under consideration includes a turbine driven by the generated steam, which requires a minimum pressure difference to operate efficiently. Fig. 12 presents the calculated average void fraction and pressure distribution along the nozzle. In these simulations, the inlet pressure and temperature were fixed at 150 kPa and 370 K, respectively, while only the outlet pressure was varied. Fig. 12a shows that the void fraction increases as the outlet back pressure decreases, because a larger pressure drop provides a stronger thermodynamic driving force for liquid–vapor phase change, leading to enhanced steam generation.

The pressure distribution (Fig. 12b) indicates that the influence of the lower outlet pressure becomes significant mainly in the downstream section of the nozzle. At lower outlet pressures, the increased steam production—together with the low density (large specific volume) of the vapor—causes the flow to expand more strongly. This expansion leads to a more pronounced pressure recovery immediately downstream of the throat, even though the overall back pressure is lower. The figure also reveals that enhanced steam production at lower outlet pressures affects the magnitude of the pressure undershoot within the nozzle. To investigate this relationship, Fig. 13 illustrates how the pressure undershoot varies with outlet pressure while keeping the inlet pressure and temperature fixed at 150 kPa and 370 K. Contrary to expectation, the results indicate that the pressure undershoot becomes less pronounced at lower back pressures. This trend can be explained by the competing mechanisms governing flashing in a nozzle. Although a lower outlet pressure increases the overall pressure drop—which promotes vapor generation—the resulting high vapor volume fraction causes strong flow

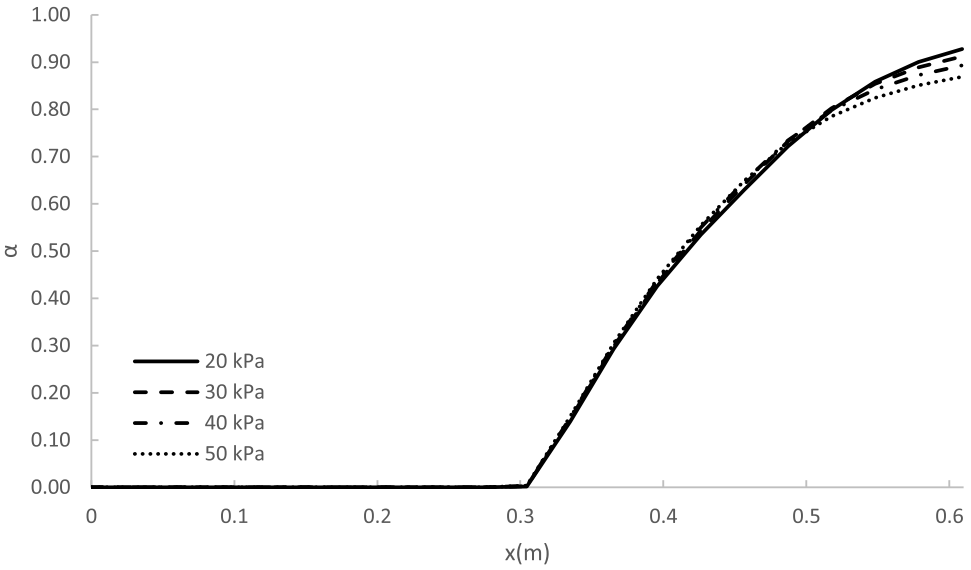

(a)

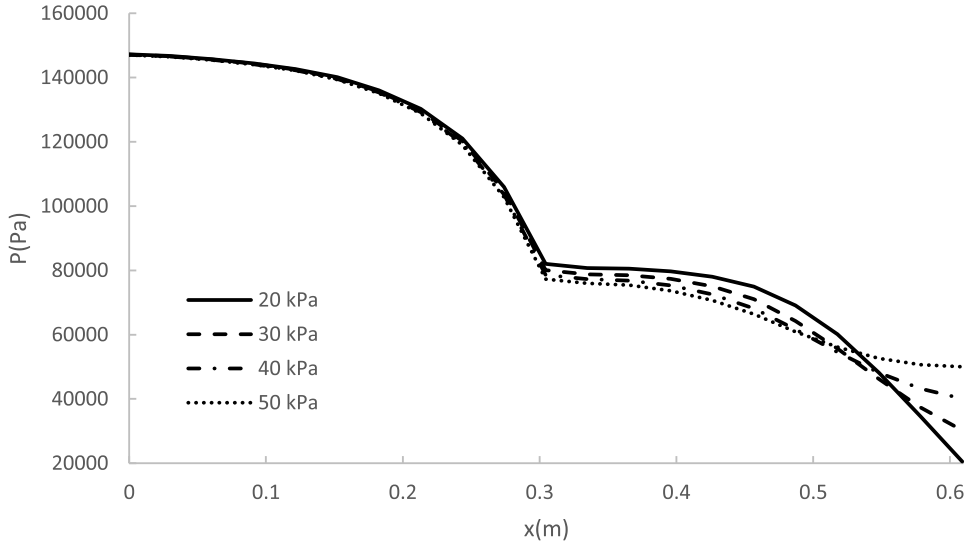

(b)

Fig. 12. Effects of the outlet pressure on (a) void fraction and (b) pressure distribution (P_{inlet}=150 kPa, T_{inlet}=370 K).

expansion and an associated pressure recovery downstream. As a result, the pressure undershoots becomes less pronounced at lower outlet pressures, despite the larger global pressure difference between the inlet and outlet.

The influence of low outlet back pressure is also evident in Fig. 14, which presents the variation of mass flow rate with outlet pressure over a range of inlet temperatures, while keeping the inlet pressure constant. The results show that the mass flow rate generally decreases at higher inlet temperatures because increased vapor generation reduces the mixture density and thus lowers the overall mass flux through the nozzle. The figure further demonstrates that, for a fixed inlet pressure, lower outlet pressures lead to enhanced steam production, which in turn reduces the mass flow rate. This indicates that simply reducing the outlet pressure does not increase throughput; instead, it enhances flashing and vapor expansion, thereby limiting the mixture mass flux.

A higher mass flow rate can be achieved by increasing the inlet pressure while keeping the other inlet and outlet conditions unchanged. Fig. 15 illustrates the effect of raising the inlet pressure from 150 kPa to 200 kPa at various outlet pressures, and a noticeable increase in mass flow rate is observed across all cases. Since the fluid enters the nozzle in a subcooled state, increasing the inlet pressure is a relatively cost-effective strategy, as it enhances both the mass flow rate and steam production while requiring only a moderate increase in pumping power.

3.3. Summary and conclusions

The Homogeneous Relaxation Model (HRM) is employed alongside a two-phase Volume of Fluid (VOF) mixture model to investigate flash

Fig. 13. Effects of outlet pressure on the pressure undershoots (P_{inlet}=150 kPa, T_{inlet}=370 K).

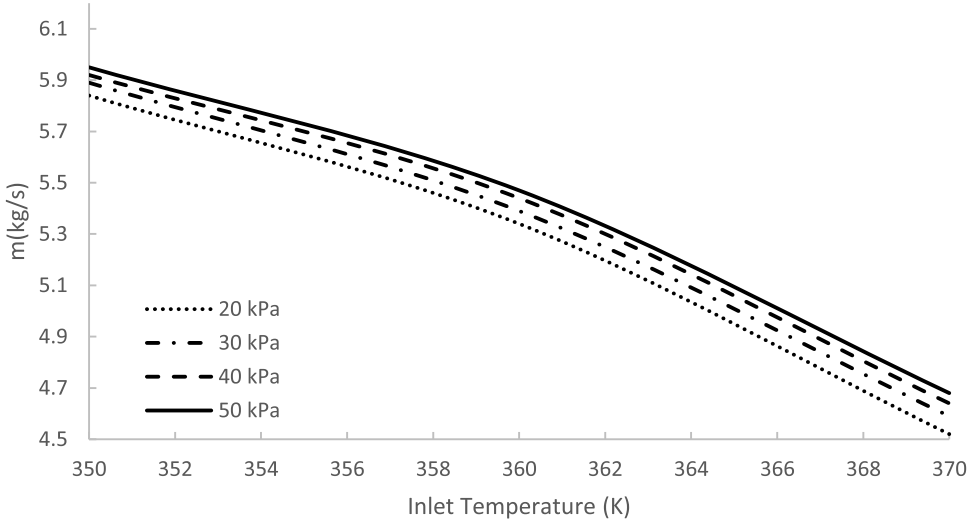

Fig. 14. Effects of outlet pressure on the mass flow rate (P_{inlet}=150 kPa).

boiling phenomena in a converging-diverging nozzle. The mass transfer between liquid and vapor phases is modelled using the Downar–Zapolski flash boiling formulation, which determines the phase change rate based on local thermodynamic conditions. The mathematical model is first validated by comparing its predictions with a benchmark experimental case from the literature. A good agreement is observed, with only a slight underestimation in the pressure recovery region of the nozzle's diverging section. Following validation, the model is applied to simulate flashing flow in the same nozzle geometry, this time with sub-atmospheric pressure imposed at the outlet. The results show that the onset of flashing occurs at the throat of the nozzle, depending on the inlet pressure and temperature. Once initiated, the void fraction increases rapidly—almost exponentially—downstream of the throat. The pressure profile exhibits a parabolic decline up to the throat, followed by partial pressure recovery toward the outlet.

The parametric study revealed that higher inlet temperatures enhance vapor formation due to the increased availability of thermal energy to drive the phase change. It was also observed that, at elevated inlet temperatures, the pressure drop within the nozzle is reduced. This behaviour is attributed to the lower specific volume of the generated vapor and the expansion driven by vapor production. The results also indicate that both inlet pressure and inlet temperature have a significant impact on the mass flow rate of the two-phase mixture in the nozzle. It is found that the mass flow rate increases substantially at higher inlet pressures, particularly when the inlet temperature is kept relatively low. This condition is advantageous for maintaining the fluid in the liquid state at the nozzle entrance, which in turn allows for the effective utilization of low-temperature waste heat sources to drive the phase change process.

The results show that the mathematical model effectively captures two critical characteristics of flash boiling in a converging-diverging nozzle: pressure undershoots and flashing delay. The pressure undershoot reflects a finite temperature difference that enables heat transfer between the liquid and vapor phases, thereby facilitating the initiation of vaporization. Simulation results indicate that pressure undershoots become more pronounced at higher inlet temperatures due to the greater superheating potential. In contrast, inlet pressure appears to have a negligible effect on pressure undershoots, which may be attributed to limitations of the current mathematical model. However, the flash delay distance is found to decrease with increasing inlet pressure,

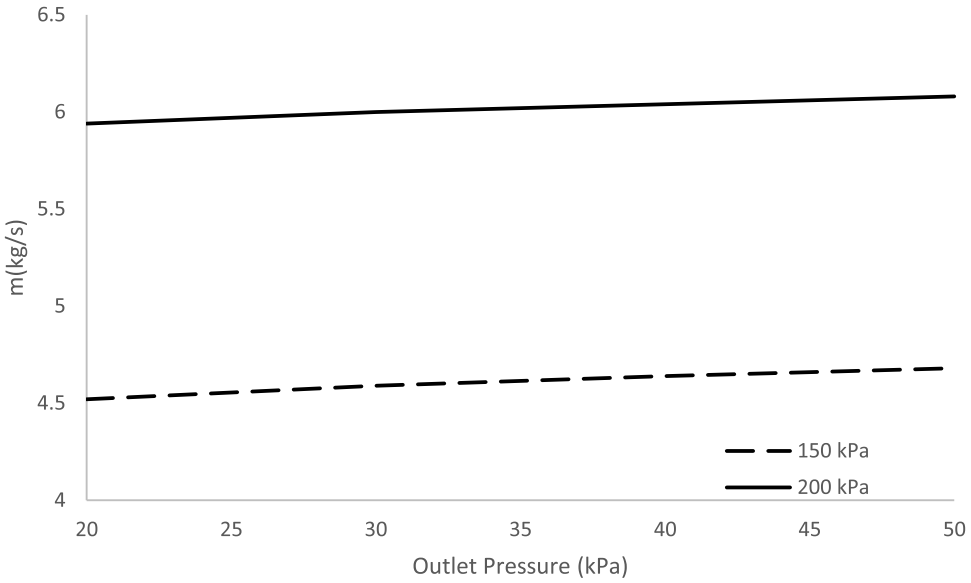

Fig. 15. Effects of inlet pressure on mass flow rate as a function of outlet pressure.

suggesting that vapor formation initiates closer to the nozzle throat under high-pressure conditions.

The effects of sub-atmospheric conditions on critical flashing parameters were investigated over a range of back-pressure values. The results show that lower back pressures promote higher steam generation due to the increased pressure difference between the nozzle inlet and outlet, which enhances the flashing potential. However, this elevated steam generation also intensifies flow expansion and pressure recovery following the onset of evaporation. Overall, the findings indicate that stronger flashing at lower back pressures results in reduced pressure undershoots and lower mixture mass flow rates. Additionally, the study confirms that the mass flow rate increases significantly with rising inlet pressure.

This study demonstrates that the Homogeneous Relaxation Model (HRM), combined with a liquid–vapor mixture model, effectively captures the key mechanisms of flashing flow in a converging-diverging nozzle. One limitation of the current approach is that HRM implicitly accounts for slip effects by incorporating both the vapor mass fraction and vapor void fraction in the calculation of the mass transfer source term. While this allows the model to approximate the relative motion between phases, it does so without explicitly solving for separate phase velocities. A more accurate prediction of void fraction could be achieved by developing and solving distinct transport equations for each phase—particularly the momentum equations—enabling each phase to evolve its own velocity field. This approach would allow direct computation of slip velocity from the velocity difference between phases, rather than relying on indirect or empirical approximations.

The study can be further improved by relaxing the adiabatic wall assumption in the nozzle. In the current model, variations in vapor temperature are primarily driven by energy exchange with the superheated liquid phase. However, under more realistic conditions involving heat transfer through the wall, wall heating or cooling can significantly influence the thermodynamic states of both the liquid and vapor phases. This, in turn, affects the extent and rate of phase change. Incorporating wall heat transfer would improve the accuracy of void fraction and vapor generation predictions, making the model more applicable to practical engineering systems.

Although this study demonstrates that the Homogeneous Relaxation Model (HRM) can be effectively used to predict the two-phase flow characteristics and phase distribution under sub-atmospheric pressures, its accuracy remains limited due to the lack of experimental validation under these conditions. An experimental setup is currently being developed in our laboratory to investigate flashing flow at sub-atmospheric pressures. The results of this future experimental work will enhance the understanding of two-phase flow behaviour in low-pressure environments and provide valuable data for further development of numerical models.

Declaration of ai-assisted technologies in the writing process

During the preparation of this work, the authors used ChatGPT to improve the readability of the manuscript. Following its use, the authors reviewed and edited the content as necessary and take full responsibility for the final version of the publication.

CRediT authorship contribution statement

Mahmut D. Mat: Writing – review & editing, Writing – original draft, Visualization, Software, Formal analysis, Data curation, Conceptualization. **Dietmar Kuhn:** Writing – review & editing, Supervision, Methodology, Formal analysis, Data curation, Conceptualization. **Abdalla Batta:** Writing – review & editing, Visualization, Formal analysis.

Declaration of competing interest

The authors declare that they have no known competing financial interests or personal relationships that could have appeared to influence the work reported in this paper.

Acknowledgement

One of the authors (Mahmut D. Mat) also gratefully acknowledges the financial support provided by the Alexander von Humboldt Foundation.

Data availability

Data will be made available on request.

References

[1] O. Miyatake, T. Tomimura, T. IDE Y Fujii, An experimental study of spray flash evaporation, Desalination. 36 (1981) 113–128.

[2] Y. Zhang, J. Wang, J. Yan, D. Chong, I. Jiping, Experimental study on energy transformation and separation characteristic of circulatory flash evaporation, Int. J. Heat Mass Transf. 99 (2016) 862–871.
[3] O. Siddiqui, Ishaq, A geothermal energy driven integrated energy system for fresh water and power production, Int. J. Hydrogen. Energy 48 (2023) 39032–39042.
[4] H. Lv, Y. Wang, L. Wu, Y. Hu, Numerical simulation and optimization of the flash chamber for multi-stage flash seawater desalination, Desalination. 465 (2019) 69–78.
[5] J. Stengler, K. Schaber, S. Mall-Gleissle, Experimental study on low temperature desalination by flash evaporation in a novel compact chamber design, Desalination 448 (2018) 103–112.
[6] M.D. Mat, H.J. Wiemer, K. Dietmar, A single stage flash power system: a practical solution for pure water production for a PEM electrolyzer plant using waste water and waste heat, Int. J. Hydrogen. Energy 191 (2025) 152313.
[7] Y. Liao, D. Lucas, Computational modelling of flash boiling flows: a literature survey, Int. J. Heat Mass Transf. 111 (2017) 246–265.
[8] Y. Liao, D. Lucas, 3D CFD simulation of flashing flows in a converging-diverging nozzle, Nucl. Eng. Des. 292 (2015) 149–163.
[9] J.P. Janet, Y. Liao, D. Lucas, Heterogeneous nucleation in CFD simulation of flashing flows in converging-diverging nozzles, Int. J. Multiphase Flow 74 (2015) 106–117.
[10] S. Mimouni, M. Boucker, J. Lavielle, D. Bestion, Modelling and computation of cavitation and boiling bubbly flows with the Neptune CFD code, Nucl. Eng. Des. 238 (3) (2008) 680–692.
[11] N. Abuaf, B. Wu, G. Zimmer, B.N. Laboratory, U.N.R. Commission, A study of nonequilibrium flashing of water in a converging-diverging nozzle, Experimental 1 (1981). NURG/CR.U.S.N.R.C.
[12] Maksic, S. Mewes D. CFD calculation of the flashing flow in pipes and nozzles, ASME 2002 Joint US-European Fluids Eng. Division Conference, Montreal, Canada 511-516.
[13] Q.D. Le, R. Merau, G. Besagni, V. Dossena, F. Inzoli, Computational fluid dynamics modeling of flashing flow in convergent-divergent nozzle, J. Fluids Eng. 140 (2018) 1–22, 101102.
[14] A.D. Le, Study of thermodynamic effect on the mechanism of flashing flow under pressurized hot water by a homogenous model, J. Fluids Eng. 144 (2022) 1–11, 011206.
[15] I.K. Karathanassis, P. Koukouvinis, M. Gavaises, Comparative evaluation of phase-change mechanisms for the prediction of flashing flows, Int J. Multiphase Flow (2017) 257–270.
[16] Z. Liu, S. Wang, Z. Lin, X. Wang, D. Wand, Y. Ouyang, D. Zhang, A non-equilibrium phase change model based on the Lee model for flashing flows in converging-diverging nozzles, Nucl. Eng. Des. 423 (2024) 113185.
[17] Bilicki Z. Kestin J. Physical aspect of the relaxation model in two phase flow. Proc. Roy Soc. London, 1990, A 428, 379-397.
[18] D.P. Schmidt, S. Gopalakrishnan, H. Jasak, Multi-dimensional simulation of thermal non-equilibrium channel flow, Int. J. Multiphase Flow 36 (2010) 284–292.
[19] Q.N. Chan, Y. Bao, S. Kook, Effects of injection pressure on the structural transformation of flash boiling sprays of gasoline and ethanol in a spark-ignition direct injection SIDI engine, Fuel 130 (2014) 228–240.
[20] C.W. Hirt, BD. Nichols, Volume of fluid (VOF) method for the dynamics of free boundaries, J. Comput. Phys. 39 (1981) 201–225.
[21] Simcenter STAR-CCM+2410 User Guide, Siemens Digital Industries Software 2025.
[22] P. Downar-Zapolski, Z. Bilicki, L. Bolle, J. Franco, The non-equilibrium relaxation model for one-dimensional flashing liquid flow, Int. J. Multiphase Flow 22 (1996) 473–483.
[23] Shih, T., Liou, W., Shabbir, A., Yang, Z. and Zhu, J. 1994. A new k-epsilon eddy viscosity model for high Reynolds number turbulent flows: Model development and validation 1994, NASA STI/Recon technical report N, 95 11442.